Applied Physics Letters

Photon helicity driven surface photocurrent in CuSe films

Cite as: Appl. Phys. Lett. **115**, 061101 (2019); https://doi.org/10.1063/1.5109069
Submitted: 06 May 2019 . Accepted: 12 July 2019 . Published Online: 06 August 2019

Gennady M. Mikheev, Vladimir Ya. Kogai, Tatyana N. Mogileva, Konstantin G. Mikheev, Aleksandr S. Saushin, and Yuri P. Svirko

Applied Physics Letters ARTICLE scitation.org/journal/apl

Photon helicity driven surface photocurrent in CuSe films

Cite as: Appl. Phys. Lett. **115**, 061101 (2019); doi: 10.1063/1.5109069
Submitted: 6 May 2019 · Accepted: 12 July 2019 ·
Published Online: 6 August 2019

Gennady M. Mikheev,[1] Vladimir Ya. Kogai,[1] Tatyana N. Mogileva,[1] Konstantin G. Mikheev,[1] Aleksandr S. Saushin,[1,2] and Yuri P. Svirko[2,a)]

AFFILIATIONS

[1]Institute of Mechanics, Udmurt Federal Research Center of the UB RAS, Izhevsk, 426067 Russia
[2]Institute of Photonics, University of Eastern Finland, Joensuu FI-80101, Finland

[a)]Author to whom correspondence should be addressed: yuri.svirko@uef.fi

ABSTRACT

We report excitation of the spin-polarized currents in CuSe nanocrystalline films and demonstrate that the inversion of the excitation photon helicity reverses the direction of the photocurrent propagating perpendicular to the plane of incidence. By performing measurements of the photocurrent propagating both along and perpendicular to the plane of incidence, we show that the observed spin-polarized currents originate from the circular surface photogalvanic effect (C-SPGE). In contrast to the conventional circular photogalvanic effect, which is associated with spin–orbit interaction and can be observed in gyrotropic media, the C-SPGE originates from the scattering of the spin-polarized charge carriers on the surface. We demonstrate that in CuSe films, the C-SPGE gives rise to the photon helicity sensitive photoresponse, making this material attractive for optoelectronics and spintronics applications.

Excitation of spin-polarized photocurrents has recently emerged as a powerful tool to study optical and electronic properties of graphene,[1] 2D dichalcogenides,[2] quantum wells,[3,4] topological insulators,[5–7] planar nanostructures,[8,9] metal, semiconductors, and composite films.[10–15] Since spin-polarized photocurrents originate from the transfer of angular momenta from photons to charge carriers, they are determined by the helicity of the excitation photons, providing unique information on the properties of the electronic ensemble.[16] In gyrotropic media, the transfer of the angular momentum manifests itself as the circular photogalvanic effect (CPGE),[17] which is associated with spin–orbit interaction that leads to the motion of spin-polarized charge carriers.[18] In a medium without the inversion center, a transfer of photon angular momentum to electrons is possible when it is accompanied by translational momentum transfer. This phenomenon is known as the circular photon drag effect (CPDE).[19] The CPDE, which manifests itself as a helicity-dependent photocurrent propagating perpendicular to the plane of incidence, has been observed in quantum wells,[20] photonic crystal slabs,[8] graphene,[21,22] bulk Te,[23] thin metal films,[10] and metal/semiconductor nanocomposites.[14,15]

It is important, however, that both CPGE and CPDE are possible in both bulk and low-dimensional materials, i.e., they produce spin-polarized currents that are not sensitive to the surface properties. At the same time, the anisotropic momentum distribution of photoexcited carriers may essentially influence their motion in the subsurface layer. The diffuse scattering of these carriers on the semiconductor surface results in the electric current.[24] This phenomenon, which is referred to as the Surface Photogalvanic Effect (SPGE), has been studied in n-GaAs,[24] polycrystalline Cu,[25] nanographite,[26,27] and metal/semiconductor nanocomposites.[28] However, until now, no circular SPGE (C-SPGE) has been reported. It is worth noting that the C-SPGE promises interesting opportunities in spintronics, allowing one to steer electron currents by optical means.

In this paper, we report on the experimental observation of the C-SPGE. We demonstrate that under irradiation with femtosecond optical pulses, the direction of transverse photocurrent generated in a thin CuSe film reverses when we switch circular polarization of the excitation beam from left- to right-handed. Having direct and indirect bandgaps of 1.43 eV and 1.02 eV, respectively,[29] CuSe shows promising photoelectric and optical properties,[29–31] being an attractive material for electronic and optoelectronic applications.[32] We demonstrate that in CuSe films, the SPGE gives rise to the polarization-sensitive photovoltage that can be used, for example, to visualize the photon helicity.

In our experiments, thin nanocrystalline CuSe films were synthesized by successive thermal vacuum deposition of thin Se and Cu layers on glass substrates at room temperature.[33] CuSe crystallites that

have a linear size of a few tens of nanometers are formed when hot Cu clusters hit the freshly grown Se film.[33] By varying the amount of Se and Cu, one can obtain a stoichiometric CuSe film with the thickness from 40 to 250 nm.

The peak at 261.3 cm^{-1}, which can be assigned to the Se-Se stretching mode,[34] dominates the Raman spectrum of the synthesized film with a thickness of 93 ± 5 nm and an average roughness of 2 nm shown in Fig. 1(a). The X-ray diffraction pattern reveals [see Fig. 1(b)] that the film consists of the hexagonal CuSe belonging to a crystallographic space group $P6_3/mmc$ with lattice parameters $a = 0.3939$ nm and $c = 1.725$ nm. The widths of diffraction peaks indicate that the average size of crystallites is about 25 nm and that they grow predominantly in the (006) plane. Since we observed no signatures of the amorphous and crystalline Se, one may conclude that the synthesized thin film consists of CuSe nanocrystallites. The film is conductive and semitransparent having a transmittance (measured relative to the glass substrate) of 37.3% at 795 nm [see Fig. 1(b), inset] and *p*-type conductivity at the sheet resistance of 30 Ω/□.

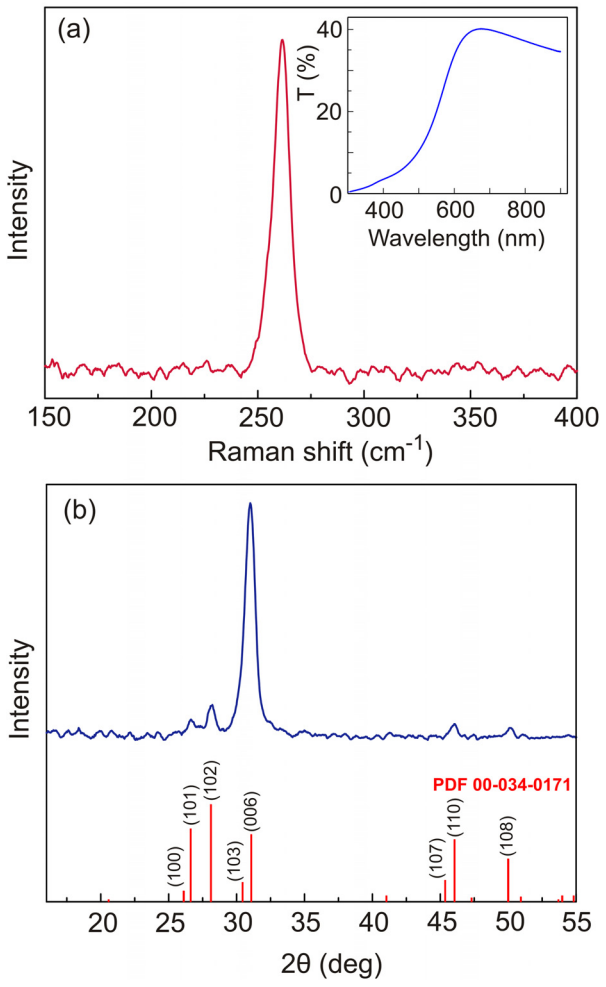

FIG. 1. (a) Raman and transmittance (inset) spectra of the synthesized film; (b) measured X-ray diffraction pattern of the synthesized CuSe film (blue solid line) and X-ray diffraction resonances of CuSe powder (PDF 00-034-0171).

To measure the photocurrent, we deposited gold electrodes along the shorter sides of the 15 × 35 mm^2 CuSe sample. The electrodes were connected to a digital oscilloscope with the bandwidth of 300 MHz. The film was irradiated with 120 fs pulses of the Ti:S laser operating at 795 nm and with the repetition rate of 1 kHz. The energy of the laser pulse varied in the range of 30–300 μJ. The photovoltage generated between electrodes did not depend on what part of the film surface is irradiated, provided that laser spot does not touch the electrodes. We found that in our measurement setup, the irradiation of the film with femtosecond laser pulses results in the photovoltage pulse with the duration less than 7 ns.

In our experiments, we measured amplitudes of the photovoltage pulses generated when the plane of incidence was perpendicular (U_x) and parallel (U_y) to the electrodes. Figures 2 and 3 show dependences of the light-to-current conversion efficiencies $\eta_{x,y} = U_{x,y}/rE_{in}$, where E_{in} is the energy of the excitation laser pulse and $r = 50\ \Omega$ is the input resistance of the oscilloscope, on the polarization azimuth Φ of the laser beam. Insets to Figs. 2(a), 2(b), and 3 present sketches of the experimental setups, in which the plane of incidence σ coincides with the XZ plane of the laboratory frame. The polarization azimuth Φ of the linearly polarized excitation beam was controlled by rotating the fast optical axis of the half-wave plate by $\delta = \Phi/2$ [see insets to Figs. 2(a) and 2(b)]. By placing a quarter-wave plate having the fast axis in the incident plane between the half-wave plate and the sample [see the inset to Fig. 3], we convert the linearly polarized beam into an elliptically polarized one with a helicity of $P_{cir} = \sin 2\Phi$.

Our measurements showed that no photocurrent is generated at normal incidence ($\alpha = 0$) regardless of the beam polarization. Similarly, no transverse photocurrent is generated at *p*- and *s*-polarizations regardless of the angle of incidence. We have also found that the sign of the photovoltage is reversed for mirrored incidence (i.e., $\eta_{x,lin}$ and $\eta_{y,lin}$ are odd functions of α) and that the photovoltage is a linear function of the laser pulse energy E_{in} independent of the polarization of the excitation beam.

One can observe from Figs. 2(a) and 2(b) that conversion efficiencies for the linearly polarized excitation beam are well described by the following equations:

$$\eta_{x,\mathrm{lin}}(\Phi) = \eta_{x,\mathrm{lin}}(\Phi = 0)\cos^2\Phi, \quad (1)$$

$$\eta_{y,\mathrm{lin}}(\Phi) = \eta_{y,\mathrm{lin}}(\Phi = 45^\circ)\sin 2\Phi. \quad (2)$$

It is worth noting that $\eta_{x,\mathrm{lin}}$ has a maximum value for the *p*-polarized (Φ = 0) and it is zero for the *s*-polarized (Φ = 90°) excitation beam. One can observe from Fig. 2(b) and Eq. (2) that the transverse photocurrent is an odd function of polarization azimuth and that it vanishes when the excitation beam is either *p*- or *s*-polarized.

Figure 3 shows the dependence of the conversion efficiency $\eta_{y,\mathrm{cir}}$ for the elliptically polarized excitation beam with a helicity of $P_{cir} = \sin 2\Phi$ on the polarization azimuth Φ (see the inset to Fig. 3) at the angle of incidence of $\alpha = 45°$. One can see from Fig. 3 that transversal photocurrent has the maximum value for the circularly polarized excitation beam and changes polarity upon helicity reversal. It is also worth noting that the transversal photovoltage vanishes for the *p*-polarized (Φ = 0) and *s*-polarized (Φ = 90°) excitation beams. The conversion efficiency obtained in the experiment is well approximated by a linear function of P_{cir},

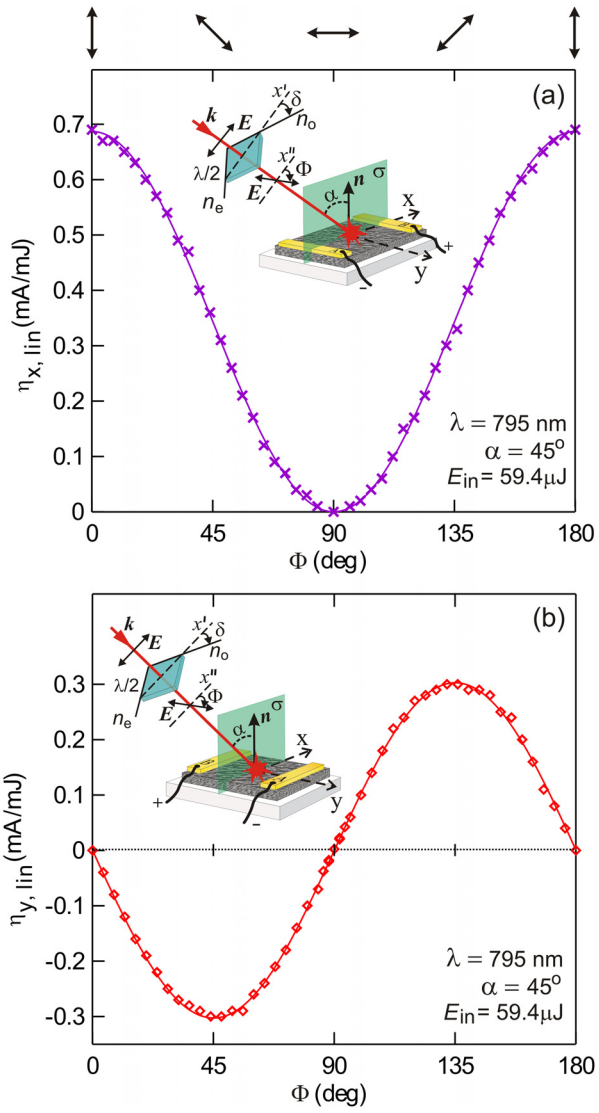

FIG. 2. Conversion efficiencies to the longitudinal $\eta_{x,lin}$ (a) and transverse $\eta_{y,lin}$ (b) photocurrents as functions of the polarization azimuth Φ at the angle of incidence of $\alpha = 45^o$. The orientation of the polarization plane is depicted at the top of the figure. The insets show the orientation of the plane of incidence σ with respect to electrodes, where x, x', and x'' axes lie in the σ plane and n_o and n_e denote the fast and slow axes of the half-wave plate. Axes of the laboratory Cartesian frame are also shown.

$$\eta_{y,cir} = \eta_{y,cir}(\Phi = 45^\circ) P_{cir} = \eta_{y,cir}(\Phi = 45^\circ) \sin 2\Phi, \qquad (3)$$

where $\eta_{y,cir}(\Phi = 45^\circ)$ is a conversion efficiency for the left-circularly polarized excitation beam. Our measurements have shown that Eqs. (1)–(3) remain valid for an arbitrary angle of incidence.

In order to reveal the underlying physical mechanism of the observed effect, it is instructive to compare data obtained in the transversal and longitudinal configurations. Specifically, since in the longitudinal configuration, a photon momentum transfers to an electron independently of polarization, the photon drag effect should produce

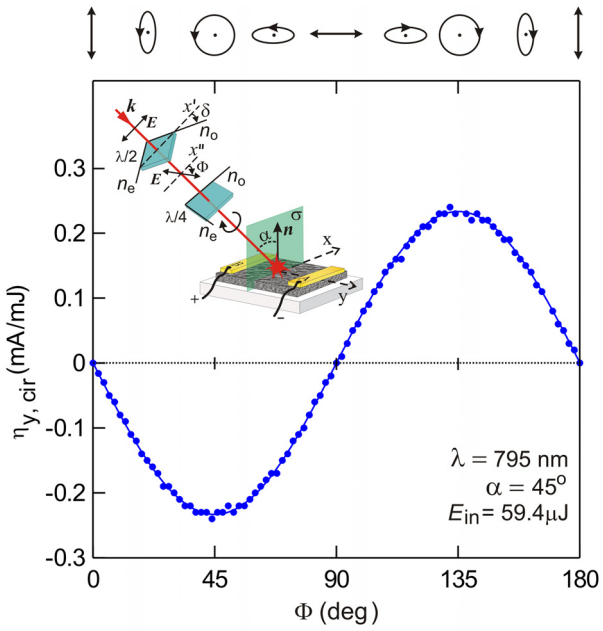

FIG. 3. Dependence of the conversion efficiency to the circular photocurrent $\eta_{y,cir}$ on the polarization azimuth $\Phi = 2\delta$ of the excitation beam before the quarter-wave plate. The polarization ellipses of the excitation beam after quarter-wave plate are shown above. The inset shows the orientation of the plane of incidence σ with respect to electrodes, and n_o and n_e denote fast and slow axes of the half-wave and quarter-wave plates. Axes of the laboratory Cartesian frame are also shown.

nonzero $\eta_{x,\,lin}$ for both *s*- and *p*-polarized excitation beams. However, in our experiment, the longitudinal photocurrent does vanish when the excitation beam is *s*-polarized, indicating that photon drag effect does not dominate the photoresponse. At the same time, polarization dependences of the longitudinal and transverse photocurrents shown in Figs. 2(a) and 2(b), respectively, are in agreement with theoretical predictions for the SPGE.[24,25] Since the excitation photon energy (1.558 eV) exceeds the CuSe bandgap, the interband transitions result in the orientation of the photoexcited electrons. If the electron momenta in the subsurface layer are oriented along the polarization azimuth of the excitation beam, the scattering rate of photoelectrons generated at the oblique incidence will be different for electrons moving toward the surface and away from the surface.[24] This asymmetry results in the SPGE, giving rise to the dependence of the photocurrent on the polarization azimuth shown in Figs. 2(a) and 2(b). It is worth noting that since the CuSe film is semitransparent, surface photocurrents are generated at the both CuSe/glass and CuSe/air interfaces.

Since the studied films are composed of CuSe nanocrystallites belonging to the nongyrotropic crystallographic space group $P6_3/mmc$, the helicity dependent transverse photocurrent presented in Fig. 3 cannot originate from the CPGE[17] and the surface CPGE.[13] Furthermore, in the semitransparent CuSe film, the CPDE should also be excluded from the list of possible mechanisms of the observed effect because photon drag results in the transversal photocurrent only when the absorption length is shorter than the electron mean free path.[15,35] These observations allow us to suggest that both longitudinal and the transverse photocurrents originate from SPGE. Therefore, the transversal photocurrent generated under irradiation with elliptically polarized

excitation beam is a manifestation of the circular SPGE (C-SPGE), which has been predicted by Magarill and Entin[36] and theoretically described by Belinicher.[37] This phenomenon originates from the asymmetry in the scattering of spin-polarized conduction electrons, which are generated by the excitation beam with nonzero helicity $P_{cir} \neq 0$ and scattered from the film surface.

In conclusion, we demonstrate a polarization-sensitive photoresponse of CuSe nanocrystalline films, which depends on the angle of incidence and polarization of the excitation laser beam. The data obtained in the longitudinal and transverse configurations allow us to conclude that the observed phenomenon originates from the surface photogalvanic effect (SPGE). We observed spin-polarized currents generated due to the circular SPGE, which manifests itself as reversal of the transversal photocurrent flow direction when the excitation beam swaps from left- to right-circularly polarized. We demonstrate that in CuSe films, the SPGE gives rise to the strong helicity-sensitive photoresponse, making this material attractive for optoelectronics and spintronics applications.

This work was supported by the RFBR (Grant No. 19-02-00112), the Academy of Finland (Grant Nos. 323053 and 298298), and H2020 MCSA DiSetCom Project.

REFERENCES

[1]M. M. Glazov and S. D. Ganichev, Phys. Rep. **535**, 101 (2014).
[2]H. Wang, C. Li, P. Fang, Z. Zhang, and J. Z. Zhang, Chem. Soc. Rev. **47**, 6101 (2018).
[3]S. D. Ganichev and W. Prettl, J. Phys.: Condens. Matter **15**, R935 (2003).
[4]E. L. Ivchenko and S. D. Ganichev, "Spin-photogalvanics," in *Spin Physics in Semiconductors*, Springer Series in Solid-State Sciences, edited by M. Dyakonov (Springer, Cham, 2017), Vol. 157, pp. 281–328.
[5]C. Kastl, C. Karnetzky, H. Karl, and A. W. Holleitner, Nat. Commun. **6**, 6617 (2015).
[6]X. Wang, Z. Miao, Y. Ma, H. Chen, H. Qian, and Z. Zha, Nanoscale **9**, 14512 (2017).
[7]Y. Q. Huang, Y. X. Song, S. M. Wang, I. A. Buyanova, and W. M. Chen, Nat. Commun. **8**, 15401 (2017).
[8]T. Hatano, T. Ishihara, S. G. Tikhodeev, and N. A. Gippius, Phys. Rev. Lett. **103**, 103906 (2009).
[9]M. Eginligil, B. Cao, Z. Wang, X. Shen, C. Cong, J. Shang, C. Soci, and T. Yu, Nat. Commun. **6**, 7636 (2015).
[10]M. Akbari and T. Ishihara, Opt. Express **25**, 2143 (2017).
[11]H. Hirose, N. Ito, M. Kawaguchi, Y. C. Lau, and M. Hayashi, Appl. Phys. Lett. **113**, 222404 (2018).
[12]A. Zhang, Q. Ma, Z. Wang, M. Lu, P. Yang, and G. Zhou, Mater. Chem. Phys. **124**, 916 (2010).
[13]Z. Zhang, R. Zhang, Z. L. Xie, B. Liu, M. Li, D. Y. Fu, H. N. Fang, X. Q. Xiu, H. Lu, Y. D. Zheng, Y. H. Chen, C. G. Tang, and Z. G. Wang, Solid State Commun. **149**, 1004 (2009).
[14]G. M. Mikheev, A. S. Saushin, and V. V. Vanyukov, Quantum Electron. **45**, 635 (2015).
[15]G. M. Mikheev, A. S. Saushin, V. V. Vanyukov, K. G. Mikheev, and Y. P. Svirko, Nanoscale Res. Lett. **12**, 39 (2017).
[16]E. L. Ivchenko, *Optical Spectroscopy of Semiconductor Nanostructures* (Springer, NewYork, 2004).
[17]V. M. Asnin, A. A. Bakun, A. M. Danishevskii, E. L. Ivchenko, G. E. Pikus, and A. A. Rogachev, Solid State Commun. **30**, 565 (1979).
[18]E. L. Ivchenko, Phys.-Usp. **45**, 1299 (2002).
[19]V. I. Belinicher, Sov. Phys. Solid State **23**, 1981 (2012).
[20]V. A. Shalygin, H. Diehl, C. Hoffmann, S. N. Danilov, T. Herrle, S. A. Tarasenko, D. Schuh, C. Gerl, W. Wegscheider, W. Prettl, and S. D. Ganichev, JETP Lett. **84**, 570 (2007).
[21]J. Karch, P. Olbrich, M. Schmalzbauer, C. Zoth, C. Brinsteiner, M. Fehrenbacher, U. Wurstbauer, M. M. Glazov, S. A. Tarasenko, E. L. Ivchenko, D. Weiss, J. Eroms, R. Yakimova, S. Lara-Avila, S. Kubatkin, and S. D. Ganichev, Phys. Rev. Lett. **105**, 227402 (2010).
[22]C. Jiang, V. A. Shalygin, V. Y. Panevin, S. N. Danilov, M. M. Glazov, R. Yakimova, S. Lara-Avila, S. Kubatkin, and S. D. Ganichev, Phys. Rev. B **84**, 125429 (2011).
[23]V. A. Shalygin, M. D. Moldavskaya, S. N. Danilov, I. I. Farbshtein, and L. E. Golub, Phys. Rev. B **93**, 045207 (2016).
[24]V. L. Al'perovich, V. I. Belinicher, V. N. Novikov, and A. S. Terekhov, Sov. Phys. JETP **53**, 1201 (1981).
[25]V. L. Gurevich and R. Laiho, Phys. Solid State **42**, 1807 (2000).
[26]G. M. Mikheev, V. M. Styapshin, P. A. Obraztsov, E. A. Khestanova, and S. V. Garnov, Quantum Electron. **40**, 425 (2010).
[27]P. A. Obraztsov, G. M. Mikheev, S. V. Garnov, A. N. Obraztsov, and Y. P. Svirko, Appl. Phys. Lett. **98**, 091903 (2011).
[28]G. M. Mikheev, A. S. Saushin, V. M. Styapshin, and Y. P. Svirko, Sci. Rep. **8**, 8644 (2018).
[29]Y.-Q. Liu, H.-D. Wu, Y. Zhao, and G.-B. Pan, Langmuir **31**, 4958 (2015).
[30]S. R. Gosavi, N. G. Deshpande, Y. G. Gudage, and R. Sharma, J. Alloys Compd. **448**, 344 (2008).
[31]X. Hou, P. Xie, S. Xue, H. Feng, L. Li, Z. Liu, and R. Zou, Mater. Sci. Semicond. Process. **79**, 92 (2018).
[32]Y. Ma, H. Ji, Z. Jin, J. Wang, X. Zheng, R. Yuan, H. Li, and S. Zhao, Integr. Ferroelectr. **181**, 102 (2017).
[33]V. Y. Kogai, A. V. Vakhrushev, and A. Y. Fedotov, JETP Lett. **95**, 454 (2012).
[34]M. Ishii, K. Shibata, and H. Nozaki, J. Solid State Chem. **105**, 504 (1993).
[35]V. L. Gurevich and R. Laiho, Phys. Rev. B **48**, 8307 (1993).
[36]L. I. Magarill and V. M. Entin, Sov. Phys. JETP **54**, 531 (1982).
[37]V. I. Belinicher, Sov. Phys. Solid State **24**, 7 (1982).